ISSN 1068-3739, Russian Meteorology and Hydrology, 2021, Vol. 46, No. 1, pp. 10–18. Allerton Press, Inc., 2021.
Russian Text The Author(s), 2021, published in Meteorologiya i Gidrologiya, 2021, No. 1, pp. 17–28.

Method for Identifying and Clustering Rossby Wave Breaking Events in the Northern Hemisphere

A. V. Gochakov[a, b]*, O. Yu. Antokhina[c], V. N. Krupchatnikov[a, b, d], and Yu. V. Martynova[b, e]

[a]*Siberian Regional Research Hydrometeorological Institute, ul. Sovetskaya 30, Novosibirsk, 630099 Russia*

[b]*Obukhov Institute of Atmospheric Physics, Russian Academy of Sciences, Pyzhevskii per. 3, Moscow, 119017 Russia*

[c]*Zuev Institute of Atmospheric Optics, Siberian Branch, Russian Academy of Sciences, pl. Akademika Zueva 1, Tomsk, 634021 Russia*

[d]*Institute of Computational Mathematics and Mathematical Geophysics, Siberian Branch, Russian Academy of Sciences, pr. Akademika Lavrent'eva 6, Novosibirsk, 630090 Russia*

[e]*Institute of Monitoring of Climatic and Ecological Systems, Siberian Branch, Russian Academy of Sciences, pr. Akademicheskii 10/3, Tomsk, 634055 Russia*

**e-mail: wandering@bk.ru*

Received August 5, 2020
Revised August 24, 2020
Accepted October 6, 2020

Abstract—Many large-scale dynamic phenomena in the Earth's atmosphere are associated with the processes of propagation and breaking of Rossby waves. A new method for identifying the Rossby wave breaking (RWB) is proposed. It is based on the detection of breakings centers by analyzing the shape of the contours of potential vorticity or temperature on quasimaterial surfaces: isentropic and iserthelic (surfaces of constant Ertel potential vorticity (PV)), with further RWB center clustering to larger regions. The method is applied to the set of constant PV levels (0.3 to 9.8 PVU with a step of 0.5 PVU) at the level of potential temperature of 350 K for 12:00 UTC. The ERA-Interim reanalysis data from 1979 to 2019 are used for the method development. The type of RWB (cyclonic/anticyclonic), its area and center are determined by analyzing the vortex geometry at each PV level for every day. The RWBs obtained at this stage are designated as elementary breakings. Density-Based Spatial Clustering of Applications with Noise algorithm (DBSCAN) was applied to all elementary breakings for each month. As a result, a graphic dataset describing locations and dynamics of RWBs for every month from 1979 to 2019 is formed. The RWB frequency is also evaluated for each longitude, taking into account the duration of each RWB and the number of levels involved, as well as the anomalies of these parameters.

DOI: 10.3103/S1068373921010027

Keywords: Rossby wave breaking, blocking, potential vortex, potential vorticity, cluster analysis

1. INTRODUCTION

Synoptic-scale eddies vortices play a key role in the mixing and transport in the middle and high latitudes. Such vortices at the initial stage of their development are formed due to baroclinic instability; at the stage of barotropic decay, a wave is broken and absorbed either in the critical layer or in front of it, which often causes an irreversible mixing of ambient air [15, 35]. The phase of such barotropic decay was called the "wave breaking" [28]. The Rossby wave breaking (RWB) is an extremely significant dynamic process in the atmospheric circulation that is connected with a number of large-scale events such as atmospheric blocking, cutoff cyclones, storm tracks, North Atlantic and North Pacific teleconnection patterns, monsoon systems [2, 6, 21, 25, 27, 33, 36, 40, 41]. In addition, the RWB processes are indirectly (through the wave energy transfer) associated with the formation of wave packets, sudden stratospheric warmings, and other processes that occur through the troposphere–stratosphere interaction [10, 26, 28, 32]. The propagation of Rossby waves is determined by the characteristics of potential vorticity (PV). When the meridional PV gra-

dient is small, high-amplitude Rossby waves can break, which leads to the PV mixing in the longitude-limited wave breaking area. In its turn, the RWB is manifested as a large-scale irreversible overturning of the contours of a potential vortex on isentropic surfaces [27]. The breaking processes are described in the framework of the theory of interaction between finite-amplitude waves and the main stream formulated in the 1970s and 1980s [5]. In the recent papers, the activity of finite-amplitude waves is determined using the deviations of potential vortex contours from the zonal symmetry [19]. Unlike in previous theories, the wave activity is easily calculated, which allows some significant simplifications.

The Rossby wave breaking is a key process in the occurrence of most westerlies blocking events. It provides a mechanism of irreversible deformation of the circulation pattern (a change in the sign of the meridional gradient of potential temperature or vortex). This mechanism is typical of blocking with a meridional inversion of the geopotential height (potential temperature) gradient typical of so called Rex blockings [22, 25, 30, 39]. The deformation of PV contours accompanied by the deep invasion of high-vorticity air masses to the tropics (or low-vorticity ones to the polar regions) during the RWB periods facilitates the formation of the abnormal pattern of weather and, in particular, of extreme events. The range and scale of weather anomalies depend, in particular, on a region and a type of wave breaking: anticyclonic (AC) or cyclonic (C) types [38], which, in turn, are determined by the jet stream features [7, 25].

In the recent decades, there have been synchronous changes both in the parameters of large-scale waves and in the number of observed weather extremes. Some studies associate the accelerated warming in the Arctic with the weaker and increasingly wavy mid-latitude westerly jet, which favors blockings with more frequent extreme events in the mid-latitudes [3, 12, 16–18, 24, 34, 42]. The authors of [20] presented an overview of publications that support a poleward shift of the Northern Hemisphere storm tracks. The authors of [4, 23, 29] demonstrate an increasing number of blocking episodes in the Northern Hemisphere in the 20th and 21st centuries. The essential changes in the key climatic parameters related to RWB, as well as an increase in the number of weather and climate extremes caused an avalanche-like increase in the interest in the variability of RWB in the Northern Hemisphere and related processes. However, a difference in the approaches to the estimation of the RWB number led different researchers to different results not only in terms of climatology of RWB zones but also in the assessment of their long-term variability. This difference is especially caused by different types of quasimaterial surfaces (isentropic and constant Ertel VP, iserthelic) used for the analysis, as well as by different methods for identifying a fact of RWB (the calculation of the gradient relative to the central latitude or the analysis of the contour geometry) [6, 9, 11, 25, 31, 37].

Let us focus on several key results obtained for the longest series in the Northern Hemisphere. In 2018, the authors of [20] showed that the AC type of RWB becomes more frequent and is shifted toward the pole, especially in summer for the isentropic surfaces of 350 and 370 K; the frequency of C type increases for the surface of 320 K. The authors of [9] demonstrated a westward shift in the AC RWBs and an increase in the C-type frequency in the North Pacific in winter and summer for potential temperature at the level of PVU (the dynamic tropopause; PVU is potential vorticity unit). The authors of [9] supposed that these changes may be associated with a change in the position of jet streams and in their relation to the RWB type. Some regional estimates of the RWB variability over Asia were obtained in [11]: a decreasing frequency of the AC RWBs was found for Central Siberia.

The present study proposes a modified method for identifying and quantifying RWBs based on two key approaches. Firstly, this is the classic determination of the RWB geometry, including the identification of the type (AC or C) [37], the center, and area of RWB. Secondly, the clustering of the centers of individual RWBs was used for the first time to identify the main RWB areas; it allows the detailed discrimination between individual RWB events during a month (or another time period). The discrimination between the RWB areas is especially urgent for the regions and seasons where the interaction between planetary waves and the polar vortex becomes maximal, and the RWB takes the most complex forms. Revising the approaches to the analysis of RWB identification, the authors primarily set the following tasks, that cannot be solved on the basis of existing RWB results:

—the objective analysis of RWB dynamics during the seasons in individual years without using synoptic charts of vorticity (for example, the problem of analyzing the cold winter of 2011/2012, the RWB analysis for extreme precipitation events in the Far East in 2013, etc.);

—the analysis of the RWB anomaly as a whole for separate months and seasons;

—the possibility of assessing long-term variability of RWB for any Northern Hemisphere regions;

—the wide access of scientific audience to the results of application of the objective method for the RWB identification.

The developed method is rather flexible and can be applied not only to quasimaterial but also to isobaric surfaces and to the description of RWBs for any region.

2. DATA AND METHODS

2.1. Data

The ERA-Interim reanalysis data with a horizontal resolution of 0.75 0.75 for 12:00 UTC were used [13]. The method is implemented using data on potential vorticity on the isentropic surface of 350 K. The algorithm is universal and, if necessary, can be used for other surfaces. The present paper demonstrates the identification of RWBs in the area of the subtropical tropopause limited by the subtropical jet stream [31]. Twenty iserthelic levels from 0.3 to 9.8 PVU with a step of 0.5 PVU were taken for the study.

2.2. Methods

Determining the RWB contour geometry. The coordinates of the potential vortex contours were determined for each PV level. The algorithm for the RWB detection is based on the method used to analyze the vortex contour geometry, with the identification of the area of multiple intersections with a beam originating from the pole point, with a step of 1 in longitude [37].

The polygon of the polar vortex contour is used as initial data in the algorithm. At the initial stage, the intersections of this polygon with the beams drawn from the pole point with the 1 step are found. While moving counterclockwise along the contour, the consecutive cases for which at least three intersection points are found, are grouped (Fig. 1a). Thus, a new group is created at the first detection of the multiple intersection of the beam with the contour and is filled with such cases till the intersection of the next beam with the contour becomes the only one. The complex geometric features of the contour (at the meridional intersection of several RWB areas) are taken into account by analyzing the latitudinal shift between the intersection points on the current and previous beams that are the closest to the pole. It should not exceed 3 . The polygon ("breaking tongue") is formed for each of these groups. The next stage consists in identifying the opening and closing points for every polygon. For this purpose, the occurrence of each point of the contour in the area of the tongue polygon is checked when passing counterclockwise along the polar vortex contour. The first phase of the occurrence is considered as an opening point, and the last case is considered as a closing point. If the latitude of the opening point (*3* in Fig. 1b) is greater than the latitude of the closing point (*4* in Fig. 1b), the type is classified as anticyclonic (AC), otherwise it is cyclonic (C; Fig. 1c).

The coordinate of the RWB center is calculated as a centroid of points determining the RWB contour (the black dot in the area *2* in Fig. 1).

The algorithm was complemented for the correct determination of the polar vortex contour features in the area of the zero meridian. For the continuous analysis of RWBs, the initial field is mirrored relative to 90° of longitude and, if the RWB that was absent due to the contour closure in the area of the zero meridian is detected, the reconstructed contour is used instead of the original one. Some conditions were added to filter insignificant areas [9]:

—the length of the contour must exceed 1500 km along the perimeter;

—the RWB area must extend for more than 5° in longitude.

The additional conditions for filtering by area according to which the contour area must be more than 500000 km^2, were also added.

Thus, at the initial stage, the following information was accumulated for every day of every month: the presence of RWB for each of 20 contours, its type, and the coordinate of its center. The whole dataset obtained at this stage was designated as elementary breaking (EB).

Clustering RWB centers. The monthly sample of EB centers in terms of spatial and temporal distances between the centers is investigated to group (cluster) events with a single center. The problem of clustering points by the distance between them is to be solved, i.e., the problem of grouping of the set of objects into subsets (clusters).

The approach is based on the DBSCAN (Density-Based Spatial Clustering of Applications with Noise) algorithm [14], with an extension for the time coordinate (ST-DBSCAN) [8]. The clusters are calculated using monthly samples of identified EBs separately for AC and C types for each year for all PV levels. The events are grouped by the distance between the geographic coordinates of EB centers using three main spatiotemporal threshold values. Two of them are: Eps1 is the threshold of spatial density (the maximum spatial distance) between two points, for which the clustering is considered; Eps2 is the temporal threshold

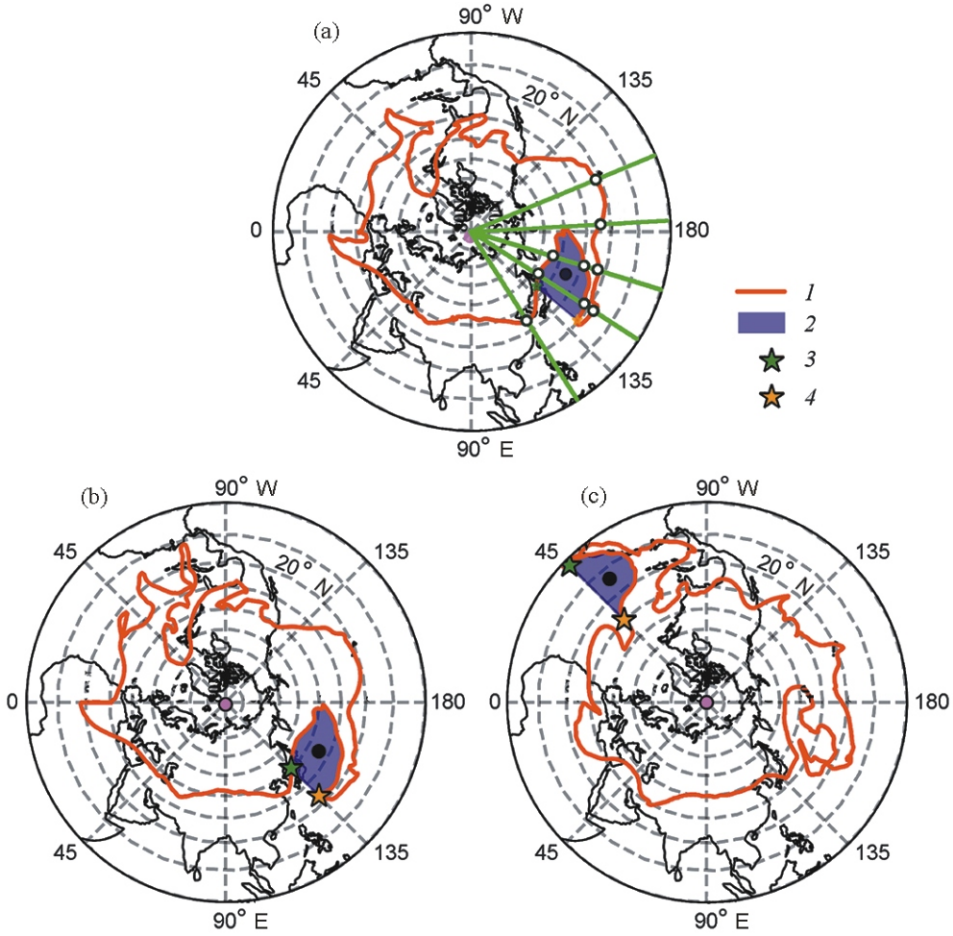

Fig. 1. (a) The graphic presentation of the algorithm for identifying Rossby wave breaking and the examples of identification of (b) anticyclonic and (c) cyclonic types of the breaking (*1*) for the iserthelic level of 1.8 PVU, (*2*) identification of the RWB zone, (*3*) the opening and (*4*) closing points.

(the maximum time interval) between two points, for which the clustering is considered. In the experiments, the threshold for the number of days was equal to the number of days in the sample (Eps2 = 31); in this case, one cluster may include points with any time interval between individual events (similar to the classic DBSCAN algorithm). For the studies of specific periods, it might be interesting to use the time distance for identifying each chain of the grouped events, proceeding from the assumption that the same event cannot have a break of several days. In this case, if the threshold for the number of days is exceeded, a new cluster is formed that unites single cases into the series of spatiotemporal unique events.

The third threshold value MinPts is the condition of considering the analyzed point as a core one; to meet this condition, at least MinPts of individual points must be achievable from the analyzed point (including itself) in the vicinity with the radius Eps1 and Eps2.

The clusters are formed of core points (determined using the MinPts condition) and points that are achievable in the maximum distance (the Eps1 and Eps2 conditions) from the core point to the neighboring points, which were not classified as core ones. The spatial density was calculated using the Chebyshev distance: the metric L in the vector space that is defined as the largest distance between the points x and y with n possible ways between them:

$$L(x,\ y) \quad \max_{i\ \ 1\ldots n} \left| x_i \quad y_i \right|.$$

Selecting clustering parameters. The presented algorithm is sensitive to the choice of conditions. This is its advantage but simultaneously causes certain difficulties in selecting parameters for different periods with different wave characteristics (a degree of the jet meandering). The most complicated task is to choose the threshold value MinPts in the case when the neighboring single events simultaneously have the fol-

lowing peculiarities: the complex shape of the same RWB, that should not be interpreted as several ones; the presence of several single RWBs in the neighboring regions caused by the baroclinity growth, that should not be interpreted as one. It was possible only to find out the optimum value of the parameters Eps1 and MinPts using the semiempirical approach. The values of one of the parameters were recorded in turn, and the variants were calculated for a number of values of the second parameter, while the results were compared with the maps of potential vorticity at the level of 350 K and with the number of EBs. For this purpose, the series of test years were used (14 in total). The parameter Eps1 was registered at the value of 400 km for both types of the breaking (which is rather close to the parameters used in [6] for other methods). For Eps1 = 400 km, the value of MinPts was selected in the range of 5 to 20 points. The result of the algorithm operation was tested for every month of every year. The number of clusters at the MinPts growth was compared with the "reference events" over the North Atlantic, Pacific Ocean, Europe, and Asia. The reference events were selected on the basis of the synoptic analysis of PV charts for the level of 350 K. Since the summer period with the greatest number of EBs over Eurasia was the most difficult, blocking diagrams obtained using the criterion from [39] were also used for some years (http://lop.iao.ru/meteo/, https://bit.ly/3kNJ7qW). The August of 2016 can be mentioned as an example, when the number of EBs was one of the highest: 1384 (the average long-term number of EBs for the period of 1979–2019 in August is 1100). The analysis of synoptic conditions and the blocking diagram revealed the frequent occurrence of RWB processes over the sector of 60 –80 E. However, high spatial density and the closeness of EBs to each other over Eurasia did not allow grouping RWBs to different clusters if using the value of MinPts below 13; if MinPts = 14, this zone was successfully separated from the RWB cluster over Europe. As soon as the algorithm captured reference breakings, the value of MinPts and the number of EBs were fixed. It turned out that the result of the algorithm operation almost did not change depending on MinPts for the months with the EB minimum (winter); however, the use of a too large number of points did not allow detecting almost any cluster. Such situation was typical of C-type EBs. Their number was much smaller than that for the AC type, and the seasonal variations were less clearly pronounced. For the summer months with the maximum of AC EBs (especially for July–September), the value of MinPts was maximal and had a rather wide range, which is determined by the vorticity configuration. The more complex it was, the higher value of MinPts was needed to distinguish the reference clusters. The relationship between the field of points for EBs and MinPts on the graph was best approximated by the second-degree polynomial smoothing (the coefficient of determination $R^2 = 0.84$). This relationship was used to choose MinPts for each range of the EB number: the maximum possible value of MinPts was selected. As a result, MinPts varied from MinPts = 5 for the number of EBs = 150–300 to MinPts = 14 for the number of EBs > 1300.

Final filtering. In some cases, the result of the clustering could contain an excessive number of clusters (this is partly associated with the selection of the maximum possible threshold of MinPts for a specific EB range). The result could also contain inessential information about RWBs that are discontinuous in time and level. In general, the portion of all filtered cases is very small at the last stage, but the filtering provides a clearer interpretation of the main results. The following procedures are applied to eliminate redundancy:

—merging the clusters distanced by not more than 15 in longitude, into a single cluster;

—removing controversial levels: if there is a break for more than two levels for an event, the most frequent set is chosen (for example, if an event is detected at the level of 4–5 PVU and, after that, only at the level of 7 PVU, only the level of 4–5 PVU is displayed);

—filtering the events that have less than three levels per one date;

—deleting artefacts: one RWB may be identified twice with different coordinates due to its complex shape. It is better to perform the removal of these artefacts in the identification algorithm (a case with the maximum area is chosen) after the clustering of EBs.

3. RESULTS AND DISCUSSION

The result is a freely distributed archive of diagrams and maps, which can be downloaded from http://sibnigmi.ru/RWB/ or https://bit.ly/30Xp95K. The archive contains the following information.

1. The section "RWB monthly visualization 1979–2019"; it presents the cluster diagrams by time and PV levels (Fig. 2a). It also provides information on the position of all clusters per month in the Northern Hemisphere (the figure is not presented).

2. The section "RWB_long-term_1979–2019"; it presents the longitude-time diagrams for the number of RWBs (Fig. 2b) obtained as follows. Based on data using which the diagrams of the corresponding type were constructed, the number of days (the maximum is 31) with RWB multiplied by the number of levels taking part in RWB (the maximum value for a month is 620) was counted in each cluster for each month.

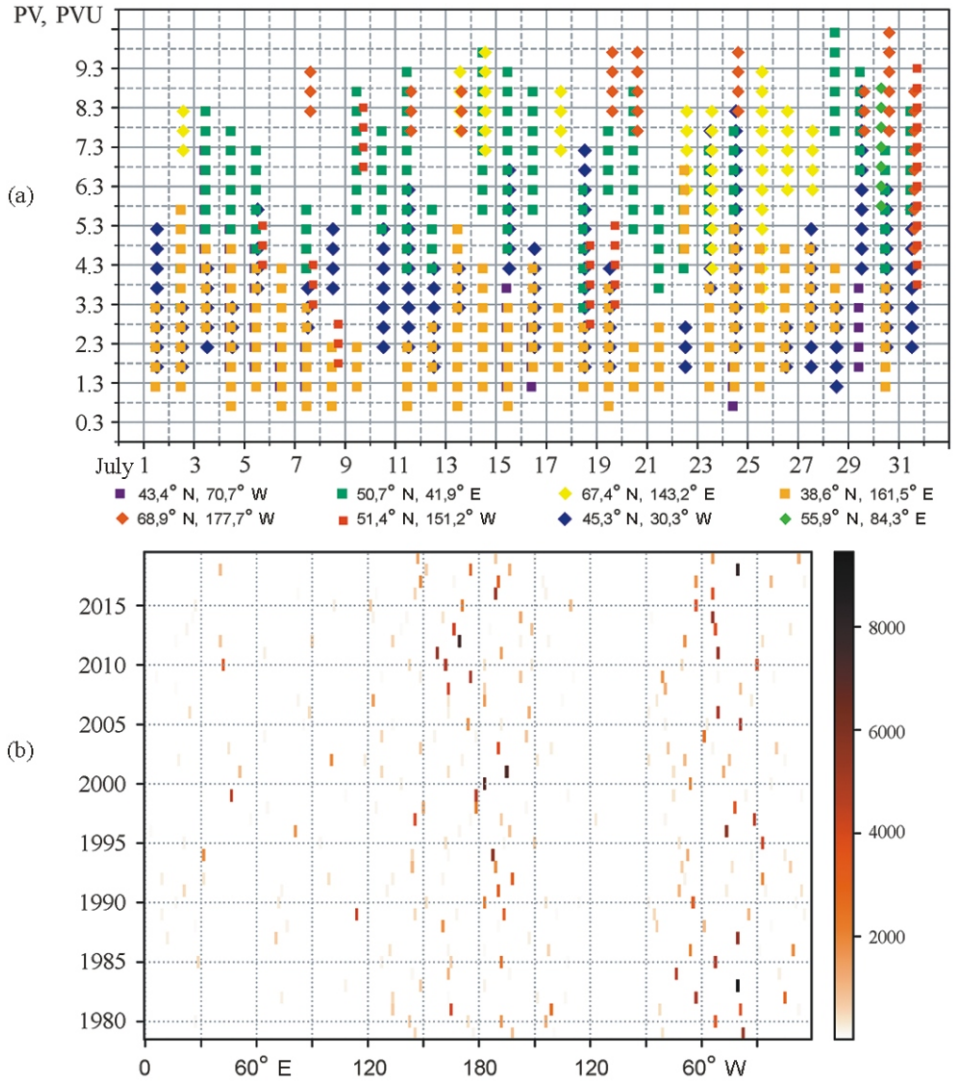

Fig. 2. (a) The diagram of the identified anticyclonic RWB clusters for every day in July 2010 for potential vorticity at the level of 350 K (the parameters MinPts = 13, EB = 1227) and (b) the longitude-time diagram of AC RWB for the whole July 2010, with account of the number of days and levels taking part in RWB (the color scale).

The consideration of the number of levels is important: the greater number of levels is involved to the breaking, the more valuable it is.

For example, Figure 2 presents the diagrams for July 2010. The summer period is of special interest here. The abnormal pattern of summer heat in the European part of Russia was associated with a very long (about two months) blocking of westerlies in the Northern Hemisphere mid-latitude troposphere [1, 3].

The authors of [1] used the methods from [30, 39] to analyze the blocking observed in 2010 in terms of RWB. In particular, it is shown that RWB was registered both in the middle and upper troposphere. However, there was a "blinking" of the wave amplitude in the tropopause area. The diagram presented in Fig. 2a leads to the conclusion that the method for the RWB identification used in the present study indicates a significant role of AC RWBs in the blocking of westerlies in July 2010 (Figure 2a shows RWBs in the cluster with the center of 59 N, 41 E (the dark green squares)).

Figure 2 demonstrates that the main RWB clusters in July 2010 were those with the centers at the longitudes of 30 W, 41 E, and 161 E. Along with the diagrams of absolute values, the diagrams of the anomalies of RWB parameters normalized by the mean value were constructed for the whole observation period and for the range of longitudes located at the distance of 10 to the left and right from the analyzed longitude (the figure is not presented). For convenience of the analysis, the archive presents both general diagrams for

the whole Northern Hemisphere and more detailed diagrams for each 90-degree longitude sector in the Northern Hemisphere.

4. CONCLUSIONS

A new method is proposed for identifying and diagnosing two types of Rossby wave breaking: anticyclonic and cyclonic. The method combines the evaluation of the shape of contours of potential vorticity (temperature) on quasimaterial (isentropic and iserthelic) surfaces and the cluster analysis. In the present paper, the method is applied to analyze RWBs at the subtropical tropopause (vorticity at the level of 350 K). As a result, the archives were obtained for every month during 1979–2019, they include the following data:

—the diagrams demonstrating the time base of RWBs with indication of the center coordinates at the levels of potential vorticity from 0.3 to 9.8 with a step of 0.5 PVU; based on these data, the Northern Hemisphere maps with the main RWB clusters per month are also presented;

—the diagrams demonstrating the long-term variability of the RWB frequency for each month. The frequency was calculated in days, with account of the number of levels for each RWB. The longitude-time diagrams are also computed for the deviation of the frequency (days and levels) from the means for the 20-degree longitude range (10 from the analyzed longitude). The diagrams are provided for the whole Northern Hemisphere, as well as for separate 90-degree sectors.

The proposed method is potentially widely scaled: different quasimaterial surfaces and characteristics used to analyze the potential vortex can be chosen for diagnosis. It should be stressed that the examples presented in the paper are a special case of the clustering algorithm selection. In the future, it is planned to extend the research domain based on the proposed method.

When using archive materials, please refer to the present article. In case you have questions on using the results presented in the archive, please contact meteosci.sibteam@gmail.com.

FUNDING

The research was supported by the Russian Science Foundation (grant 19-17-00248 “Hydrodynamic Instability and Large-scale Vortex Dynamics of the Atmosphere in a Changing Climate”). The testing of the DBSCAN algorithm parameters was partly supported by the infrastructure of Zuev Institute of Atmospheric Optics (Siberian Branch of Russian Academy of Sciences) developed and operating according to the Governmental Assignment AAAA-A17-117021310142-5, including the Atmosfera Common Use Center.

REFERENCES

1. A. R. Ivanova, N. P. Shakina, E. N. Skriptunova, and N. I. Bogaevskaya, “Comparison of Dynamic Characteristics of the Summer 2010 Blocking Anticyclone with Earlier Episodes,” in *Analysis of Abnormal Weather Conditions in Russia in the Summer 2010*, Ed. by N. P. Shakina (Triada LTD, Moscow, 2011) [in Russian].
2. I. I. Mokhov, “Action as an Integral Characteristic of Climatic Structures: Estimates for Atmospheric Blockings,” Dokl. Akad. Nauk, No. 3, **409** (2006) [Dokl. Earth Sci., No. 6, **409** (2006)].
3. I. I. Mokhov, “Specific Features of the 2010 Summer Heat Formation in the European Territory of Russia in the Context of General Climate Changes and Climate Anomalies,” Izv. Akad. Nauk, Fiz. Atmos. Okeana, No. 6, **47** (2011) [Izv., Atmos. Oceanic Phys., No. 6, **47** (2011)].
4. I. I. Mokhov and A. V. Timazhev, “Atmospheric Blocking and Changes in Its Frequency in the 21st Century Simulated with the Ensemble of Climate Models,” Meteorol. Gidrol., No. 6 (2019) [Russ. Meteorol. Hydrol., No. 6, **44** (2019)].
5. D. G. Andrews and M. E. McIntyre, “Planetary Waves in Horizontal and Vertical Shear: The Generalized Eliassen–Palm Relation and the Mean Zonal Acceleration,” J. Atmos. Sci., No. 11, **33** (1976).
6. E. A. Barnes and D. L. Hartmann, “Detection of Rossby Wave Breaking and Its Response to Shifts of the Midlatitude Jet with Climate Change,” J. Geophys. Res. Atmos., No. D9, **117** (2012).
7. P. Berrisford, B. J. Hoskins, and E. Tyrlis, “Blocking and Rossby Wave Breaking on the Dynamical Tropopause in the Southern Hemisphere,” J. Atmos. Sci., No. 8, **64** (2007).
8. D. Birant and A. Kut, “ST-DBSCAN: An Algorithm for Clustering Spatial-temporal Data,” Data & Knowledge Eng., No. 1, **60** (2007).
9. K. A. Bowley, J. R. Gyakum, and E. H. Atallah, “A New Perspective toward Cataloging Northern Hemisphere Rossby Wave Breaking on the Dynamic Tropopause,” Mon. Wea. Rev., No. 2, **47** (2019).

10. J. G. Charney and P. G. Drazin, "Propagation of Planetary-scale Disturbances from the Lower into the Upper Atmosphere," J. Geophys. Res., No. 1, **66** (1961).
11. D. Chyi, Z. Xie, N. Shi, P. Guo, and H. Wang, "Wave-breaking Features of Blocking over Central Siberia and Its Impacts on the Precipitation Trend over Southeastern Lake Baikal," Adv. Atmos. Sci., No. 1, **37** (2020).
12. J. Cohen, J. C. Furtado, J. Jones, J. A. Screen, M. Barlow, D. Whittleston, D. Entekhabi, D. Coumou, J. Francis, K. Dethloff, and J. Overland, "Recent Arctic Amplification and Extreme Mid-latitude Weather," Nature Geoscience, No. 9, **7** (2014).
13. D. P. Dee, S. M. Uppala, A. J. Simmons, P. Berrisford, P. Poli, S. Kobayashi, U. Andrae, M. A. Balmaseda, G. Balsamo, P. Bauer, P. Bechtold, A. C. M. Beljaars, L. van de Berg, J. Bidlot, N. Bormann, C. Delsol, R. Dragani, M. Fuentes, A. J. Geer, L. Haimberger, S. B. Healy, H. Hersbach, E. V. Hylm, L. Isaksen, P. Kellberg, M. Kohler, M. Matricardi, A. P. McNally, B. M. Monge-Sanz, J.-J. Morcrette, B.-K. Park, C. Peubey, P. de Rosnay, C. Tavolato, J.-N. Thepaut, and F. Vitart, "The ERA-Interim Reanalysis: Configuration and Performance of the Data Assimilation System," Quart. J. Roy. Meteorol. Soc., No. 656, **137** (2011).
14. M. Ester, H.-P. Kriegel, J. Sander, and X. Xu, "A Density-based Algorithm for Discovering Clusters in Large Spatial Databases with Noise," in *Data Mining and Knowledge Discovery* (1996).
15. S. B. Feldstein and I. M. Held, "Barotropic Decay of Baroclinic Waves in a Two-layer Beta-plane Model," J. Atmos. Sci., No. 22, **46** (1989).
16. J. A. Francis and S. J. Vavrus, "Evidence Linking Arctic Amplification to Extreme Weather in Midlatitudes," Geophys. Res. Lett., **39** (2012).
17. P. Groisman, H. Shugart, D. Kicklighter, G. Henebry, N. Tchebakova, E. Kukavskaya, S. Maksyutov, E. Monier, G. Gutman, S. Gulev, J. Qi, J. Chen, A. Prishcherov, B. Porfiriev, A. Shiklomanov, T. Loboda, N. Shiklomanov, S. Nghiem, K. Bergen, J. Albrechtova, M. Shahgedanova, A. Shvidenko, N. Speranskaya, A. Soja, K. De Beurs, O. Bulygina, J. Mccarty, Q. Zhuang, and O. Zolina, "Northern Eurasia Future Initiative (NEFI): Facing the Challenges and Pathways of Global Change in the Twenty-first Century," Progress in Earth and Planetary Science, No. 1, **4** (2017).
18. D. E. Horton, N. C. Johnson, D. Singh, D. L. Swain, B. Rajaratnam, and N. S. Diffenbaugh, "Contribution of Changes in Atmospheric Circulation Patterns to Extreme Temperature Trends," Nature, No. 7557, **522** (2015).
19. C. S. Y. Huang and N. Nakamura, "Local Finite-amplitude Wave Activity as a Diagnostic of Anomalous Weather Events," J. Atmos. Sci., No. 1, **73** (2015).
20. P. Jing and S. Banerjee, "Rossby Wave Breaking and Isentropic Stratosphere-troposphere Exchange during 1981–2015 in the Northern Hemisphere," J. Geophys. Res. Atmos., No. 17, **123** (2018).
21. W. K. M. Lau and K.-M. Kim, "The 2010 Pakistan Flood and Russian Heat Wave: Teleconnection of Hydrometeorological Extremes," J. Hydrometeorol., No. 1, **13** (2012).
22. H. Lejenas and H. Okland, "Characteristics of Northern Hemisphere Blocking as Determined from a Long Time Series of Observational Data," Tellus A, No. 5, **35** (1983).
23. A. R. Lupo, R. J. Oglesby, and I. I. Mokhov, "Climatological Features of Blocking Anticyclones: A Study of Northern Hemisphere CCM1 Model Blocking Events in Present-day and Double CO_2 Concentration Atmospheres," Climate Dynamics, No. 3, **13** (1997).
24. A. R. Lupo, I. I. Mokhov, G. Chendev, M. G. Lebedeva, M. Akperov, and J. A. Hubbart, "Studying Summer Season Drought in Western Russia," Adv. Meteorol., **2014** (2014).
25. G. Masato, B. J. Hoskins, and T. J. Woollings, "Wave-breaking Characteristics of Midlatitude Blocking," Quart. J. Roy. Meteorol. Soc., No. 666, **138** (2012).
26. T. Matsuno, "A Dynamical Model of the Stratospheric Sudden Warming," J. Atmos. Sci., No. 8, **28** (1971).
27. M. E. McIntyre and T. N. Palmer, "A Note on the General Concept of Wave Breaking for Rossby and Gravity Waves," Pure and Appl. Geophys. PAGEOPH, No. 6, **123** (1985).
28. M. E. McIntyre and T. N. Palmer, "Breaking Planetary Waves in the Stratosphere," Nature, No. 5935, **305** (1983).
29. I. I. Mokhov, A. V. Timazhev, and A. R. Lupo, "Changes in Atmospheric Blocking Characteristics within the Euro-Atlantic Region and Northern Hemisphere as a Whole in the 21st Century from Model Simulations Using RCP Anthropogenic Scenarios," Glob. Planet. Change, **122** (2014).
30. J. L. Pelly and B. J. Hoskins, "A New Perspective on Blocking," J. Atmos. Sci., No. 3, **60** (2003).
31. G. A. Postel and M. H. Hitchman, "A Climatology of Rossby Wave Breaking along the Subtropical Tropopause," J. Atmos. Sci., No. 3, **56** (1999).
32. R. S. Quiroz, "The Association of Stratospheric Warmings with Tropospheric Blocking," J. Geophys. Res., No. D4, **91** (1986).
33. J. A. Renwick and J. M. Wallace, "Relationships between North Pacific Wintertime Blocking, El Niño, and the PNA Pattern," Mon. Wea. Rev., No. 9, **124** (1996).
34. S. D. Schubert, H. Wang, R. D. Koster, M. J. Suarez, and P. Y. Groisman, "Northern Eurasian Heat Waves and Droughts," J. Climate, No. 9, **27** (2014).

35. N. Shi, X. Wang, L. Zhang, and H. Xu, "Features of Rossby Wave Propagation Associated with the Evolution of Summertime Blocking Highs with Different Configurations over Northeast Asia," Mon. Wea. Rev., No. 7, **144** (2016).
36. A. J. Simmons and B. J. Hoskins, "Barotropic Influences on the Growth and Decay of Nonlinear Baroclinic Waves," J. Atmos. Sci., No. 8, **37** (1980).
37. C. Strong and G. Magnusdottir, "Tropospheric Rossby Wave Breaking and the NAO/NAM," J. Atmos. Sci., No. 9, **65** (2008).
38. C. D. Thorncroft, B. J. Hoskins, and M. E. Mcintyre, "Two Paradigms of Baroclinic-wave Life-cycle Behavior," Quart. J. Roy. Meteorol. Soc., No. 509, **119** (1993).
39. S. Tibaldi and F. Molteni, "On the Operational Predictability of Blocking," Tellus A, No. 3, **42** (1990).
40. E. Tyrlis and B. J. Hoskins, "The Morphology of Northern Hemisphere Blocking," J. Atmos. Sci., No. 5, **65** (2008).
41. G. Wolf and V. Wirth, "Diagnosing the Horizontal Propagation of Rossby Wave Packets along the Midlatitude Waveguide," Mon. Wea. Rev., No. 8, **145** (2017).
42. X. Zhang, C. Lu, and Z. Guan, "Weakened Cyclones, Intensified Anticyclones and Recent Extreme Cold Winter Weather Events in Eurasia," Environ. Res. Lett., No. 4, **7** (2012).